RESEARCH PAPER

Investigation of the Effect of Radiosensitization of Tungsten Oxide Nanoparticles on AGS Cell Line of Human Stomach Cancer in Megavoltage Photons radiation

Amin Hassanvand [1], Mohammad Hossein Zare [1,*], Ali Shams [2,*], Abolfazlal Nickfarjam [1], Masood Shabani [3], Hossein Rahavi [2]

[1] *Department of Medical Physics, Faculty of Medicine, Shahid Sadoghi University of Medical Sciences, Yazd, Iran*

[2] *Department of Immunology, Faculty of Medicine, Shahid Sadoghi University of Medical Sciences, Yazd, Iran*

[3] *Department of Radiation therapy-Oncology, Faculty of Medicine, Shahid Sadoghi University of Medical Sciences, Yazd, Iran*

ARTICLE INFO

ABSTRACT

Radiotherapy consisting of external beam radiotherapy (EBRT) and internal radioisotope therapy (RIT) has a wide application for treating cancer as clinical trials. This study provides some conditions to prove that tungsten oxide nanoparticles (WO3) is a radio sensitizer. The peripheral blood mononuclear cells (*PBMCs*) were used to calculate inhibitory concentration (IC). The AGS cell line exposed the concentration of 89.6 μg/mL (IC_{20}) WO3 nanoparticles that was optimal and its radio sensitization was examined in megavoltage photons radiation of 6 MV x-rays. The sensitivity enhancement ratio (SER) and dose enhancement factor (DEF) was determined 1.24 and 1.68 respectively. We described the mechanisms of creating WO3 nanoparticles toxicity and genotoxicity in different concentrations on AGS cell line. The mean size of WO3 NPs by transmission electron microscopy was measured 31.89±3.82 nm. Tungsten oxide Nanoparticles cause to reduce cell viability, remove membrane and damage to DNA. There was a meaningful increasing in damages to DNA and proliferation cell potency and also significantly reducing cell viability in concentrations more than 100 μg/mL.

INTRODUCTION

Operation is a standard treatment for the most cancers; however in many cases, other treatment methods like Chemotherapy and radiation therapy are used because of inappropriate situation of tumor, existence of various tumors or when the patient prefers not to operate [1, 2].

At the moment, cancer is the second factor for death after cardiovascular disease [3]; and among the usual cancers, gastric cancer has been known as a kind of cancer with a high death rates (about 70%) whose prevalence in men is two times more than women and has more prevalence in East Asian countries.

In 2010 the amount of gastric cancer was 21000 in USA whose 10570 patients died [4].

Operations, chemotherapy and radiation therapy are three main methods for cancer treatment. Operation is an aggressive treatment in which tumor and in some cases, the whole related organs are removed. In chemotherapy, some medicines are used for destruction of cells which have more ability for cell division; this function may lead to destroy some other normal cells. In

* Corresponding Author Email: mzare6777@yahoo.com

radiation therapy, ionizing radiations is used for destruction of cancer cells which leads to damage normal cells in the radiation field, too. Based on this, it's not practically possible to increase the dose of radiation in radiation therapy[5] and for improving the treatment index, some complexes which cause to increase the radiation protection of a healthy tissue and radio sensitivity of tumor tissue[6] are used.

In many cases, the effective mechanism of sensitization complexes is to produce free radical such as ROS.

A lot of studies have been done about different physical and chemical complexes of sensitizations [7-9] in which Nano complexes have special situation and we can point to gold nanoparticles, carbon nanotubes, and metal nanoparticles [9, 10] among them.

Nanoparticles are formed from a set of atoms and molecules with different sizes and shapes, and are synthesized by different methods and the most biological processes like making a cancerous cell in Nano scale. The researchers' attempt for treating cancer has motivated them to design tools in Nano scale and entering the living cells [11].

Nano materials have a key role in damaging DNA, destruction of membrane and finally cell death by creating stress oxidative and lipid peroxidation. It can turn into an effective method for treating which leads to remove tumors by minimizing the side effects of treatment.

Increasing free radicals because of creating stress oxidative in cell environment can cause to activate necrosis and apoptosis and accordingly leads to cell death [12, 13]. Some scientists believe that the main share of heavy nanoparticles megavoltage energies like tungsten is the produced auger electron cascade due to high atomic number (Z=74) against low effective atomic number of the soft tissue (Z=7.4)(14) which has a direct relationship with Z^3. Others believe that its reason is high share of photoelectric phenomenon. Some others believe Paired production phenomenon can make difference in energies more than 10 MV.

Metal nanoparticles are radio sensitization in two energies of KV and MV, but there are two problems [15]: first, there is no assurance that these particles are biocompatible in Nano scale. Studies on pure metal nanoparticles showed that they suggested different toxicity according to their size and morphology.

The second reason is that we need high atomic number metals for radio sensitization which induce these toxicity metals; this toxicity will be more in higher concentrations of treatment.

Tungsten is a good representative for high Z radio sensitization because it's one of the heaviest metals in periodic table. On the other hand, its oxygenation form causes to be a good biocompatible[16].

In recent years, tungsten oxide nanoparticles (WO₃) has been paid more attention because it has biophysical conditions such as bigger surface area, high thermal stability and showing magnetic property[17]; however the information about the toxicity of tungsten oxide nanoparticles is limited. For example, a study [18]has been done about the cell line A549, human epithelial colorectal adenocarcinoma cells examined the toxicity of 11 metal oxide nanoparticles in direction of WO₃ NPs and toxicity was observed in high concentration (>100 μg/ mL).

Tungsten oxide nanoparticles has a high capability in X-ray absorption Coefficient and emitting Compton electrons, scattered photons, photoelectrons, and Auger electrons in high radiation energies and also in tunable localized surface Plasmon resonance in the visible and near infrared (NIR) range[19]. These features which are used for the cancer diagnosis and treatment, have caused PTT, PDT, radiotherapy, and CT imaging.

A mixture use of these methods caused to improve a mouse survival fraction.

Using the database SEER relates to cancer happening, patient's surviving and cancer prevalence in USA. Information obtained from the analysis method of Kaplan-Meier is divided into 2 categories: One of them relates to operation of gastric cancer without radiotherapy and the second is operation with radiotherapy which causes to increase the lifetime of patients after the operations[20].

Such conditions are establishing for chemo radiation therapy, of course the radiotherapy is a supplementary process for gastric cancer and is often used for prohibiting of tumor relapse.

According to the above statements, the radio sensitization of cell line of human stomach cancer in the presence of tungsten oxide nanoparticles has been studied in this study, according to nanoparticles capability in producing free radical and also tumor tissues capability in trapping nanoparticles because of high Angiogenesis.

At the end, Dose Enhancement factor (DEF)

and Ratio Sensitivity enhancement (SER) and toxicity of nanoparticles (IC_{20}) will be calculated.

The toxicity of tungsten oxide nanoparticles is also calculated for peripheral blood mononuclear cells (PBMCs (because the nanoparticles shouldn't damage these high sensitive cells which have important roles in immune system of the body if it wants to reach this clinical stage. Peripheral blood mononuclear cells (PBMCs) include lymphocytes (T, B, natural killer [NK] cell) and monocytes which play key roles in controlling the inflammation.

MATERIALS AND METHODS
Preparation of WO₃ nanoparticles

Tungsten oxide Nanoparticles were bought with diameter 23-65 nm (US-Nano, US). Tungsten oxide nanoparticles in the solution of RPMI 1640 medium (Sigma, US) has been Sonics by probe sonication (Ultrasonic technology development, IR) in 50 °c and 400 *W* of power for 30 minutes. During sonication, the surroundings of beaker were filled by ice so that the plate temperature doesn't go up too much. The accuracy of doing sonication was examined by Beer-Lambert law. The obtained solution (1 mg/mL) was stored in a cool and dark place after crossing the filter (0.2μm) in 1.5 mL microtubes and had been vortexes before each application.

Characterization of WO₃ NPs

Nanoparticles phase purity and structure were determined by X-ray diffraction (XRD) and by using Holland Philips X-ray powder diffraction (Cu Kα, λ=1.5406 Å). The average crystallite size (*L*) is calculated by using the Scherer's formula $L= 0.9λ / βcos(θ)$, where $λ$ is the wavelength of the X-ray radiation, θ and $β$ are the Bragg angle and the full width at half maximum (FWHM) of the corresponding peak. Morphological features and structure of WO₃ nanoparticles were observed by transmission electron microscopy (TEM). The samples were prepared as mounting a drop of the solutions on a carbon-coated Cu grid. Then the drop was permitted to be dried in the air. After that, the samples were observed by TEM.

Ultraviolet-visible absorption spectroscopy was performed in a double beam Spectrophotometer (Unico,US). The tungsten oxide nanoparticles at wavelength range (300-800 nm) were used for examining the suitable synthesis. There was culture media in a Quartz Cuvette and

nanoparticles at a concentration of 100 μg/ml in another Quartz Cuvette.

The specific surface area was calculated by the BET method. This method was based on the absorption isotherm of nitrogen at 77 *K* using Belsorp mini II (BEL, JAP).

The elemental composition of the prepared nanoparticles was characterized by energy dispersive spectroscopy (EDS).

Culture and cell line

AGS cell line of human stomach cancer was bought (Pasteur, Iran) and grew in RPMI-1640 cell culture media and 1% penicillin-streptomycin. The cells were incubated at 5% CO_2 and 95% air.

Isolation of PBMCs by Ficoll-Paque density gradient centrifugation

First, we poured some drops of Heparin with 5000 I.U. /mL concentration into falcon tube 50 mL. Then we added it the female blood isochoric, Phosphate-buffered saline (PBS). After that, we selected 15 mL falcon tube, poured on it the Ficoll-Paque PLUS and added diluted blood isochoric slowly. Then it was centrifuged by 1800 rpm of revolutions for 30 minutes.

We took the created white halo and poured it into the 15 ml falcon tube. We added PBS twice. It was centrifuged by 1800 rpm revolutions for 30 minutes. We dissolved the obtained sediment in 2 mL of RPMI-1640 medium including 10% FBS and 1% penicillin – streptomycin.

TEM analysis of cells with internalized WO₃ nanoparticles

$2×10^5$ AGS cells were cultured. The tungsten oxide nanoparticles were added after 24 hours. Then the cells have been washed twice by phosphate-buffered saline (PBS) and the trypsin cells are fixed in 1% tetroxide osmium, some slices were cut as 50-60 nm by ultra-microtome and were put on copper grids, and the image was taken by transmission electron microscopy (Zeiss, Germany).

Cellular viability assay

As was noted above, first of all 5000 AGS cells and 10^5 PBMCs were cultured in 96-well plates for reviewing the toxicity of WO₃ nanoparticles and gaining optimal concentration according to IC_{20} index, and the concentrations of 0,50,100 and 200 μg/mL were added to each well. The

MTT assay was done after 48, 72 and 96 hours. All measurements were done as triplicate.

It was added to each well in each plate which contained 200 μl of culture media, 20 μL MTT solution (Sigma-Aldrich, USA) at a concentration of 5mg/ml by 4 hours incubation. The reaction was stopped by removing MTT solution and adding 100 μl dimethyl sulfoxide (DMSO) (Sigma-Aldrich, USA) to each well in order to dissolve the Formazan crystals.

As it was said, AGS cells were cultured. 5000 cells were cultured in 96-well plates and grew. After 80% confluence, cells were incubated with or without nanoparticles for 24 hours. The concentration of nanoparticles was 89.6 μg/mL (IC$_{20}$). Then the plate exposed to radiation by 6 MV photons. Doses of 2, 4, 6 and 8 Gy were used. Cells' survival was examined by MTT assay one week after the radiation.

The value of absorption in wavelength 570 nm was read by micro plate reader (BioTek,US). The measurements were triplicate for AGS and PBMCs.

The percentage of cell survival will be obtained by using the following formula:

$$\text{Cell viability (\%)} = \frac{A}{B} \times 100 \qquad (1)$$

Where, A is the sample reading and B is the reading of control group and IC20 was calculated.

Cellular proliferation assay

As it was said, at first 5000 AGS cells and 10^5 PBMCs were cultured in 96-well plates in order to examine the toxicity of WO$_3$ NPs and the concentrations of 0,50, 100 and 200 μg/mL were added to each well. The BrdU assay was done after 48, 72 and 96 hours. The percentage of cell proliferation will be obtained by using the eq (1).

The BrdU assay was done by using kit (Cell signaling Technology, US) according to the manufacturer's instructions.

All measurements were done in 450 nm wavelength as triplicate. As it was said, AGS cells were cultured. 5000 cells in 96-well plates were cultured and grew.

After 80% confluence, cells were incubated with or without nanoparticles for 24 hours. The concentration of nanoparticles was 89.6 μg/ML. Then the plate exposed to radiation by 6 MV photons. Doses of 2, 4, 6 and 8 Gy were used. The cell proliferation was examined by BrdU assay one week after the radiation.

Clonogenic assay

2×10^4 AGS cells were cultured in 6-well plates and grew. After 80% confluence, the cells were incubated with or without nanoparticles for 24 hours.

The concentration of nanoparticles was 89.6 μg/mL. Then, the plate exposed to radiation by 6 MV photons. Doses 2, 4, 6 and 8 Gy were used. The cells were trypsinized and counted after the plate radiation and 1000 cells were cultured in T-75 flasks. The numbers of clones which have more than 50 cells were calculated after 14 days to estimate survival fraction.

The survival curves were fitted to the Linear Quadratic (LQ) Model that is:

$$\text{SF}(D) = \exp - (\alpha D + \beta D^2). \qquad (2)$$

D is a radiation dose in Gy and α is the cell kill per Gy of the linear component and β is the cell kill per Gy^2 of the quadratic component. The value of plating efficiency (PE) was obtained from the following relation:

$$\text{PE} = \frac{\text{Number of colonies counted}}{\text{Number of cells seeded}} \qquad (3)$$

The value of survival fraction (SF) was obtained from the following relation:

$$\text{SF} = \frac{\text{Number of colonies counted}}{\text{Number of cells seeded} \times \text{PE}} \qquad (4)$$

The sensitization enhancement ratio (SER) and dose enhancement factor (DEF) were calculated to quantify the radio sensitizing effect of the cells.

The SER factor which is given by:

$$SER_{NP} = \frac{MID_{Cont}}{MID_{NP}}. \qquad (5)$$

Where $MID = \int_0^\infty SF(D)\, dD$ and the subscripts NP and Cont refer to nanoparticles and control (radiation alone).

The DEF factor described by:

$$\text{DEF} = \frac{\text{Dose of } 2Gy\,(no\,NP)}{\begin{array}{c}\text{Dose requierd to produce in tset samples}\\ (\text{with } NP)\text{the same SF as in control with } 2Gy\end{array}} \qquad (6)$$

Apoptosis assay

Apoptosis detection was performed using the Annexin V-FITC/propidium iodide (PI). Apoptosis Detection Kit (Mabtag, Germany) was bought.

2×10^4 AGS cells were cultured in 6-well plates.

After 80% confluence, the cells were incubated with or without nanoparticles for 24 hours. Then, the 6-well plates were exposed to radiation by 6 MV photons. Doses 2, 4, 6, 8 Gy were used. Flow cytometry was done according to protocol after 4 days. The cell numbers of each sample were 10000 cells.

First, 10% binding buffer was prepared. Then the cells were trypsinized from 6-well plates and poured into the 15 mL falcon tube and were centrifuged in 1800 rpm. Then, the solution was taken and 90 μL binding buffer were added and the suspension was prepared. Then the suspension was poured into the 0.5 mL microtube and we added 5 μL PI and 5 μL Annexin V. We kept the microtube in a dark place for 20 minutes, then we added 400 μL binding buffer to the microtube and centrifuged it in the revolutions of 400 g for 5 minutes. We evacuated the above liquid and added 200 μL binding buffer to the microtube and immediately analyzed the created suspension by flow cytometry.

We examined the effect of WO_3 nanoparticles without any radiation for AGS and PBMCs. The cells were incubated in 6-well plates by nanoparticles after culturing and flow cytometry was done after 4 days.

Irradiation setup

Perspex Phantom (Fig. 1A) was designed for radiation to 96-well plates and 6-well plates. Each
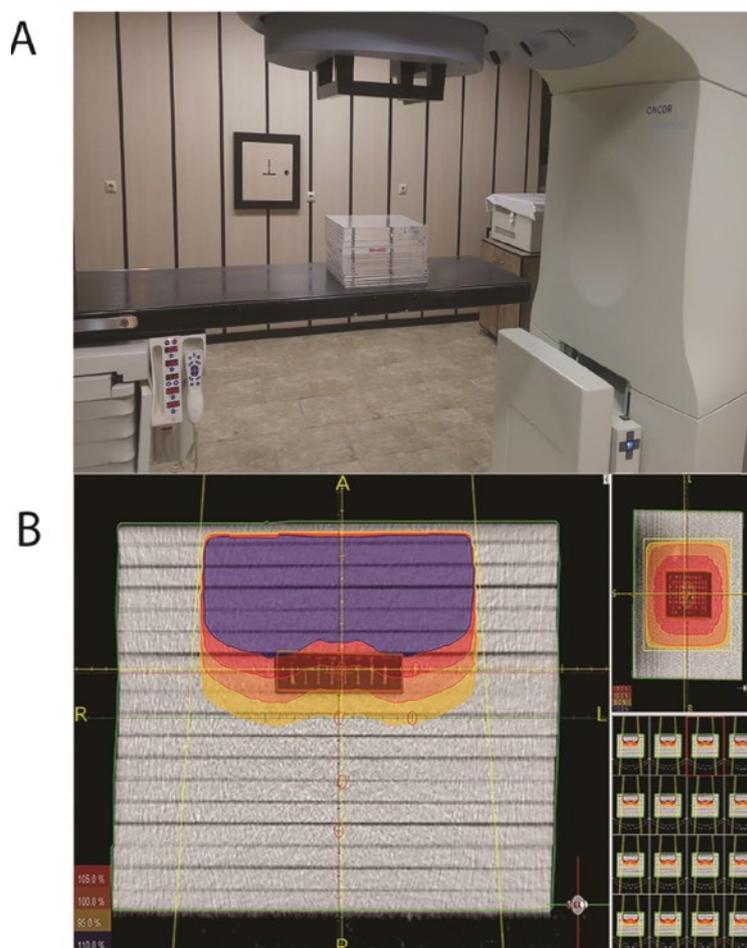

Fig. 1. Irradiation system (A) Multi-well micro plates containing the AGS cell are ready for in vitro tests. The AGS cells containing fresh medium alone or supplemented with 89.6μg/mL of WO₃ NPs were seeded into low-attachment multi-well plates.
Perspex phantom containing a micro titer plate was located on the treatment couch of the ONCOR Digital Medical Linear Accelerator, the same machine is used in daily clinical practice for the patients' radio therapeutic treatment and is subjected to specific quality assurance checks. (B) A CT scan was done in the set-up phase of the phantom containing the micro plate (in which wells were filled with culture medium) to optimize dose delivery, exactly the same as it's done for a patient. The irradiation system has ensured the delivery of a uniform dose to the yellow areas containing the micro plate, free of any doses. A Prowess Panther radiation therapy planning system was applied and customized with the geometric and dose-metric characteristics of an ONCOR Digital Medical Linear Accelerator.

well of 6-well plates included 2 mL culture media as well as AGS cell with or without nanoparticles and 6 wells of 96-well plates included 200 µL of culture media and AGS cell with or without nanoparticles. 6 wells of the plate center 96-well included the media of cell culture and the rest were filled with distilled water in order to distribute a suitable dose.

The phantom sizes were 17×30×30 cm³ including 17 slabs by 1 cm thickness and a hole was considered in the middle of phantom for plates. 11 slabs were under the plate for generate maximum backscatter.

A build-up of 6 cm Perspex was used for 6 MV photons. The applied doses were 2, 4, 6 and 8 Gy. Cells were treated in 6 MV photons (dose rate 300 MU/min).

Megavoltage X-ray (6 MV) irradiations were performed using an ONCOR Digital Medical Linear Accelerator from Siemens·

The sizes of used field were 20×24 cm² and used source surface distance (SSD) was also 100 cm.

The delivered dose was calculated using the Prowess Panther TPS that is a 3D radiation therapy treatment planning system (Philips Healthcare, DA Best, and Netherlands).

The dose distribution was calculated (Fig. 1B) on a CT data-set of the Perspex phantom with plate previously scanned on Prowess Panther CT.

Dual AO/EB fluorescent staining

$2×10^4$ AGS cells were cultured in 6-well plates. After 80% confluence, the cells were incubated with or without nanoparticles for 24 hours. Then, the 6-well plates were exposed to radiate by 6 MV photons. Doses 2, 4, 6 and 8 Gy were used. Then the cells were trypsinized from 6-well plates and poured into the 15 mL falcontube and were centrifuged in 1800 rpm, the solution was taken and 25 µL of the suspension was prepared and the suspension were transferred to glass slides·

Dual fluorescent staining solution (1µl) containing 100 µg/ml AO and 100 µg/ml EB (Sigma, US) was added to each glass slide·

Then, 500 cells of each sample were counted by fluorescent microscope (Zeiss, Germany) and we calculate the death cells according to the following index:

$$\text{Death cells (\%)} = \frac{\text{Total number of apoptotic cells and necrotic cells}}{\text{Total number of initial cell}} \times 100 \quad (7)$$

All the measurements were done as triplicate.

Statistical analysis

Two-way ANOVA followed by a Tukey post hoc test, has been used for specifying the statistical significance. All data were expressed as mean ±
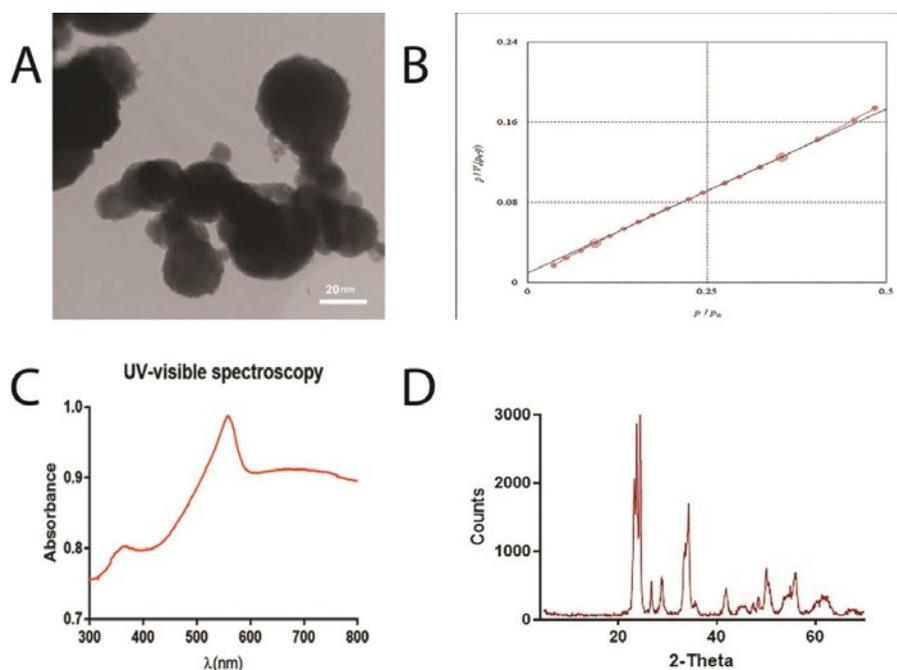

Fig. 2.Characterization of tungsten oxide nanoparticles. The TEM image of WO₃ NPs (A).(B) BET plot of WO₃ NPs. (C) XRD pattern of WO₃ NPs(D) The UV-vis spectra of WO₃ NPs in this study.

standard deviation. A p< 0.05 value has significantly been suggested differently.

RESULTS AND DISCUSSION
Nanoparticles characterization

TEM images showed that the average size of WO_3 NPs was 31.89 ± 3.82 nm and it was approved that their morphology was spherical (Fig. 2A). The specific surface area and surface area to volume ratio (SA/V) of WO_3 NPs was calculated as 12.932 m^2/g and 92.59×10^6 m^{-1} by analyzing BET, respectively (Fig. 2 B).

The NPs were characterized by XRD analysis to determine the crystalline structure.The structure of WO_3 NPs considered as the orthorhombic structure is based on the JCPDS 20-1324 standard card. The size of crystal nanoparticles was 27.72 nm calculated by using Scherer's formula at $2\theta = 24.48°$(Fig. 2C).

UV–visible spectroscopy showed absorption peaks at 560 nm for Wo_3 NPs in accordance with the characteristic surface Plasmon resonance absorption bands and relates to WO_3 NPs (Fig. 2D).

The EDS profile of WO_3 nanoparticles (Fig. 3) indicates that the sample contains tungsten, with oxygen.

Potential of metal NPs toxicity have more relationship with its physical features (21-23). Some of these features like size, shape, surface area, purring, morphology and mixture play a main role in toxicity. According to the past studies, sonication causes to reduce the Nano suspension density and to minimize the effects of surface charges[24].

The surface area has a close relationship with the size of nanoparticles. As particle size decreases, the surface area per unit volume (or mass) increases. The potential chemical interaction will be increased by raising the numbers of surface atoms and molecules[25].

When the surface area of nanoparticles increases, the numbers of free radicals and metal ions from the nanoparticles surface will be increased. These ions will have an opportunity for interacting with the cells[25, 26].

Surface area to volume ratio in nanoparticles have a significant effect on the nanoparticles properties.

This factor will be increased by reducing the nanoparticles radius for spherical nanoparticles, and as a result, the numbers of atoms and molecules in the surface of nanoparticles will be increased.

Intracellular localization of WO₃ NPs

The localization of WO_3 NPs inside AGS cells were examined by using TEM (Fig. 4A), which were aggregated and mainly localized in the
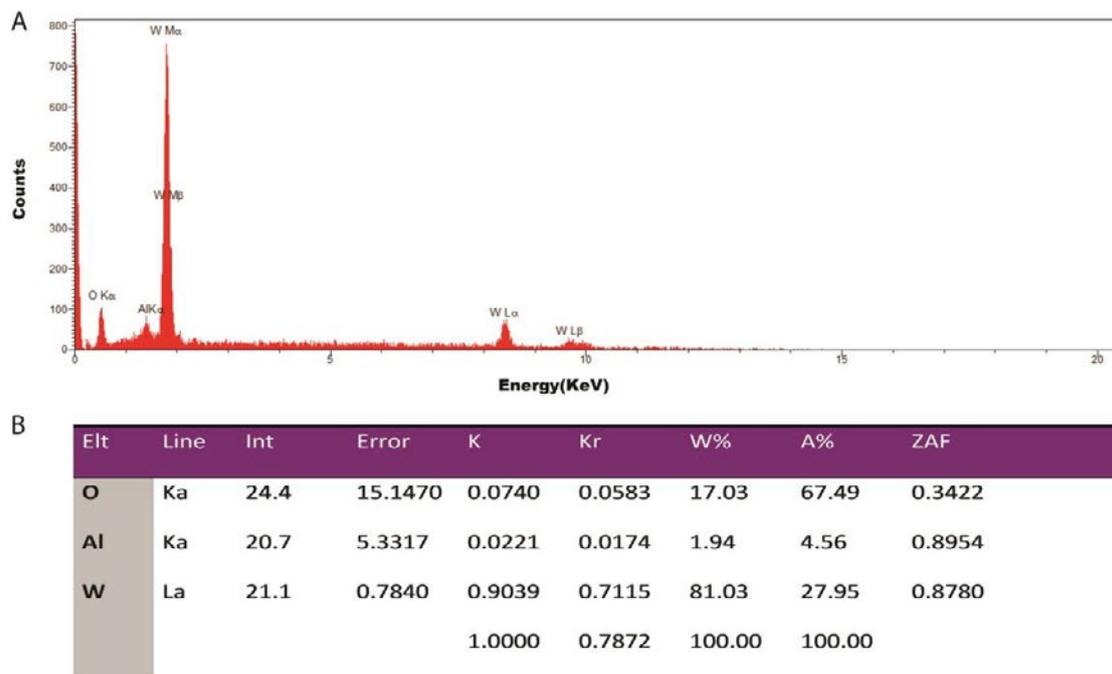

Elt	Line	Int	Error	K	Kr	W%	A%	ZAF
O	Ka	24.4	15.1470	0.0740	0.0583	17.03	67.49	0.3422
Al	Ka	20.7	5.3317	0.0221	0.0174	1.94	4.56	0.8954
W	La	21.1	0.7840	0.9039	0.7115	81.03	27.95	0.8780
				1.0000	0.7872	100.00	100.00	

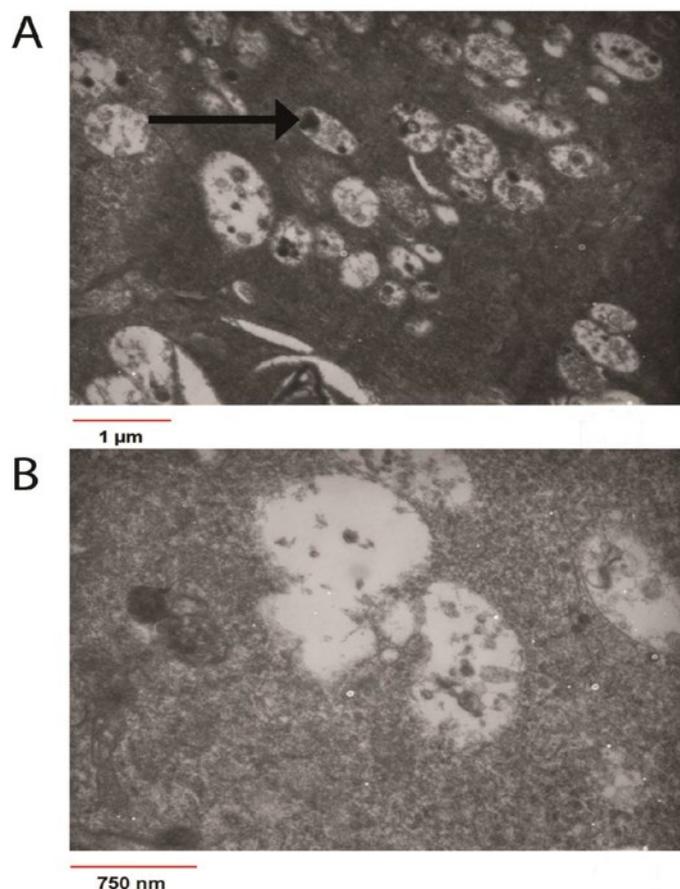Fig. 3. EDS profile of WO_3 nanoparticles and quantitative analysis.

Fig. 4. Localization of WO$_3$ NPs in AGS cells
The representative TEM image of AGS cells treated with 89.6 µg/mL WO$_3$ NPs for 24 hours, have been shown in (A). (B) The representative of TEM image in controlling the AGS cells.
Nanoparticles mainly aggregates in Endosomes obviously as black and electron-dens spots have been shown by arrow.

endosomes. The WO$_3$ NPs enter the cells most likely via endocytosis. The cells not exposed to nanoparticles were selected as control group (Fig. 4B). As it has been showed the WO$_3$ nanoparticles have put into the cell in optimal concentration.

Cytotoxicity and Genotoxicity

AGS cells and PBMCs were exposed to different concentrations (0, 50,100 and 200 µg/mL] of WO$_3$ NPs for 48, 72 and 96 hours. The toxicity of nanoparticles was examined by MTT assay (Fig. 5 A and B).

The tungsten oxide NPs induced a meaningful decrease in cell viability which was 83.69±3.455 (%), 83.09±1.563 (%) for AGS cells at 100 and 200 µg/mL concentrations for 96 h, respectively and these values were 79.7±2.214 (%) and 71.21±1.555 (%) for PBMCs, respectively. This value was 92.92±0.6825 (%) at 50 µg/mL concentration of

for AGS cells and was 84.46±3.382 (%) for PBMCs at 96 h.

IC$_{20}$ for PBMCs measured by MTT assay, was 89.6 µg/mL in 96 hours (Fig. 5 C). At last, the concentration lower than 89.6 µg/mL was offered for human cases since PBMCs were sensitive; and by using the IC$_{20}$ index, 89.6 µg/mL Concentration was selected as the optimal concentration.

BrdU assay used for quantitative examination of DNA replication is a sign of the AGS cells proliferation ability (Fig. 5 E and D).

Statistical analysis showed that the genotoxicity of nanoparticles increased noticeably in concentrations more than 50µg/mL in 48, 72 and 96 hours which caused to reduce the ability of cell proliferation for AGS cells. The amount of reducing cell proliferation ability depends on time and nanoparticles concentration so that the proliferation ability will remarkably be decreased

by raising time and nanoparticles concentration. The effect of nanoparticles concentration is more than the spent time. The ability of relative proliferation for AGS cells and PBMCs for 96 h at 200 µg/mL concentration was 12.28% and 3.74 % less than 50 µg/mL concentration for 96h and was also 28.15% and 12.43 % less than the control group, respectively.

According to some bio-distribution reports, the amount of tungsten particles distributed throughout gut in the bone marrow and peripheral blood cells, will cause genotoxicity, [27].

The studies about toxicity of WO$_3$ NPs on humans have a lot of limitations. Some of metal oxide NPs can make toxicity and cause apoptosis through ROS[28].

Due to information limits in biological interaction of tungsten oxide nanoparticles, this article tries to describe the mechanisms of creating toxicity and genotoxicity on cell line of human stomach cancer (AGS) by WO$_3$ nanoparticles as well as examining the radio sensitization of WO$_3$ NPs.

The data shows that there is a direct relationship between the concentration of WO$_3$ NPs and creating toxicity and apoptosis of AGS cell line.

Some ways were used for measuring the toxicity of WO$_3$ NPs in order to overcome this information limits. MTT assay shows the damage rate of mitochondrial activity; and BrdU assay suggests the cell proliferation ability and increasing DNA. Both ways show that a remarkable toxicity and genotoxicity of nanoparticles will be increased in concentrations over 100µg/mL.

Similar studies have been done for examining the effect of toxicity metal oxide NPs (chromium oxide, cobalt iron oxide, TiO$_2$, ZnO$_2$ and CeO$_2$) in
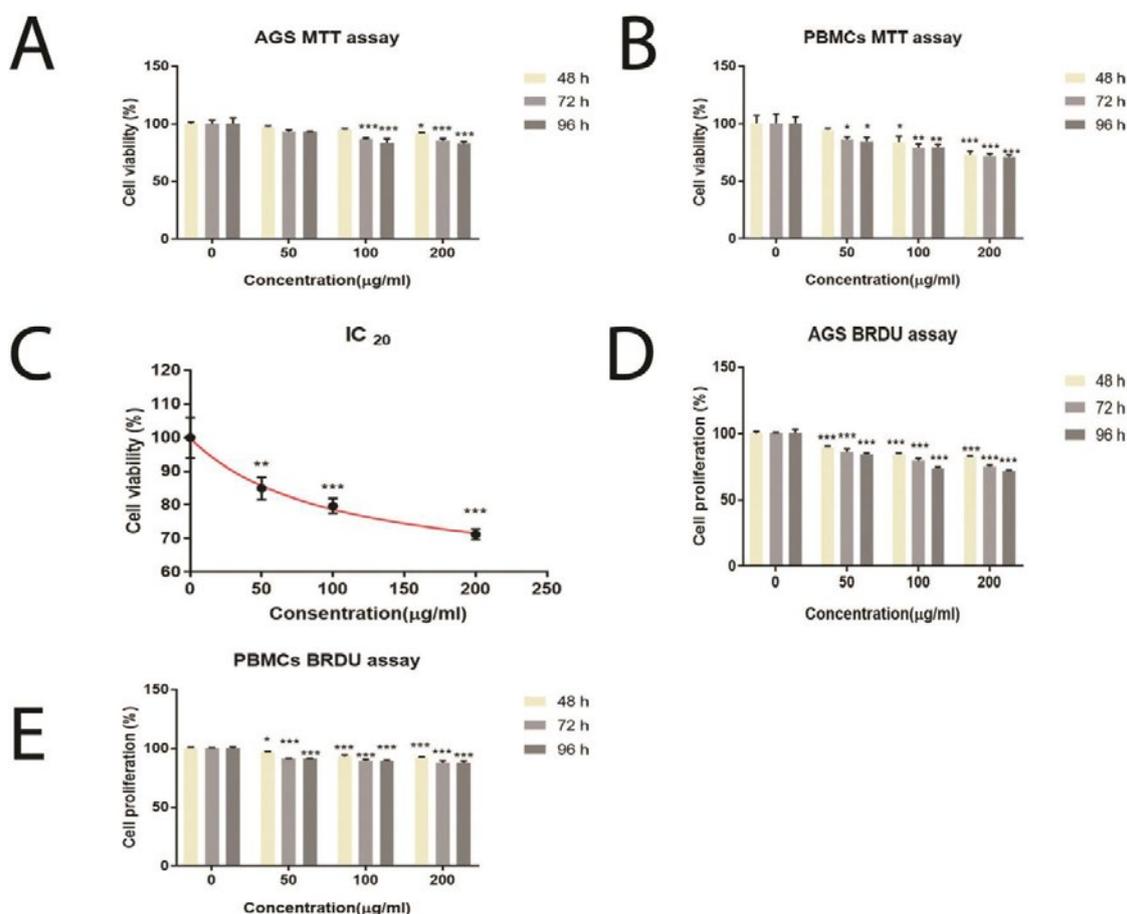

Fig. 5. By using an MTT assay and BrdU assay respectively, cell viability and cell proliferation have been specified. MTT assay of AGS cells (A), PBMCs (B) and BrdU assay of AGS cells (D) and PBMCs (E) at 48, 72, and 96 h. AGS cells and PBMCs treated by WO$_3$ NPs with different concentrations (50,100 and 200 µg/mL).(C)The IC$_{20}$ of PBMCs was 89.6 µg/mL for 96 hours, which were measured by MTT assay. Data is a summary of three independent experiments and expressed as mean ± SD. *P<0.05, **P<0.01, ***P<0.001 compared with the control group.

high concentration based on the results [29-31]. In a similar study, the production of ROS in high nanoparticles concentrations was the reason for making stress oxidative and cell toxicity. High production of ROS causes cell damage through oxidizing cell biomolecules such as antioxidant GSH, CAT and oxidant MDA levels which have a main role in keeping redox homeostasis.

In the recent studies, a remarkable increase was observed in DNA damage concentrations more than 200 µg/mL of WO₃ NPs. The small size and large surface area caused to increase damaging DNA.

Our results show that genotoxic WO₃ NPs capability for damaging DNA has a noticeable increasing in high concentrations (≥100 µg/mL).

WO₃ NPs capability for making toxicity in different concentrations was examined. The results of the genotoxicity test in cultured rat liver cells showed that 8-oxo-2-deoxyguanosine levels increased significantly [32].

The results showed that ROS production can cause genotoxicity by increasing activation of different directions like chromosomal aberrations or double strand in the nucleus. This study was approved by researches on kidney cells exposed to nanoparticles ZnO for 24 hours and led to increase in damaging DNA.

Tungsten oxide nanoparticles can cause the genotoxic effects through direct and indirect interaction with DNA including oxidative stress and apoptotic responses. However Caspase has an important role in damaging DNA[33].

Caspases are a family of Aspartic protease which have cysteine and play a key role in cell apoptosis.

In the recent studies, it was suggested that ROS accumulation produced by nanoparticles led to create apoptosis in the concentrations between 200 and 300 µg/mL, has more remarkable increase than the control group. Changes in penetrability of Mitochondrion is the reason for the apoptosis.

Caspase-9 and -3 has a main role in damaging DNA[34] and cell death by segmenting cell protein. The loss of caspases or failure in their performances can lead to cancer.

Based on the reports, we understand that CeO₂, Mn₂O₃ and Co₃O₄ NPs dissolution was very low although WO₃, CuO and ZnO NPs dissolution was rather high [35, 36]. Our results approved these reports, too. However the stability of WO₃ NPs in RPMI-1640 medium was 48 hours. Zinc oxide nanoparticles have toxicity because of its high solubility in a rather low concentration but tungsten oxide nanoparticles has no toxicity although its solubility is comparable.

Zinc metal nanoparticles create more toxicity in humans than tungsten metal nanoparticles [37]. In the performed research, it was specified that soluble nanoparticles of metal oxide must have toxic Cations so that it can create toxicity. Evidence suggests that free ions can enter the
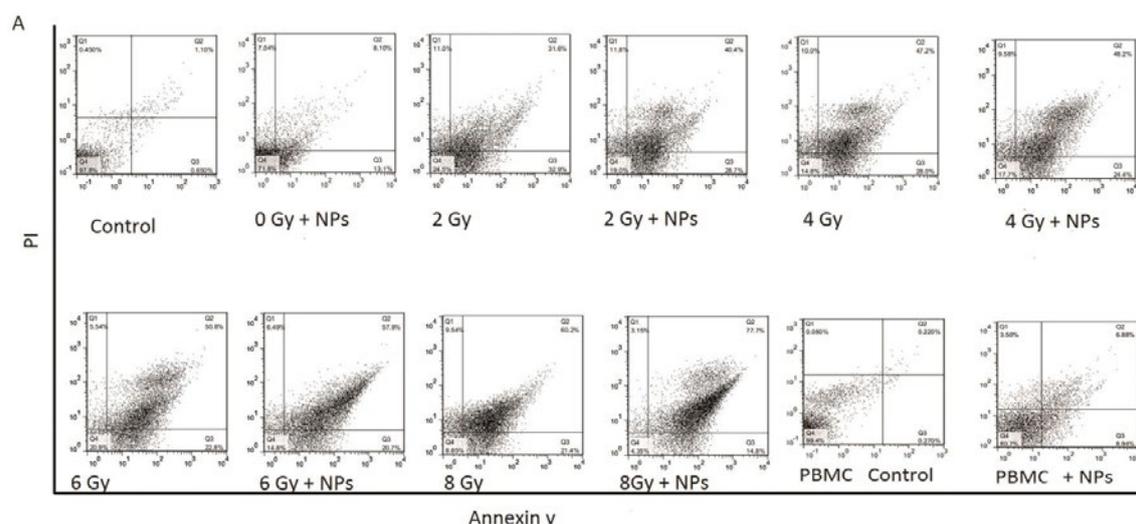

Fig. 6. Flow cytometer analysis of apoptosis in AGS cells And PBMCs with Annexing V and PI staining. The AGS cells apoptosis rates and PBMCs followed by 2,4,6 and 8 Gy of irradiation have treated with or without 89.6 µg/mL WO₃ NPs. Apoptosis in AGS cells and PBMCs have been showed in this figure: first apoptotic cells (lower-right quadrant, Annexing V+/PI-) and secondary apoptotic and necrotic cells (upper-right quadrant, Annexing+/PI+).

cells better than nanoparticles. On the other hand, Cations W don't do this action contrary to Cations Z which interact by Zn^{2+}-dependent enzymes and transcription factors[38]. The loss of toxic ions can be the reason for non-toxicity of WO₃ NPs. As it was reported, Tungsten oxide have anti-bacterial activity against bacteria like Gram-positive and Gram-negative Bacteria.

The performed studies show that anti-bacterial activity of tungsten oxide will be increased by reducing the size of nanoparticles and increasing the H$^+$ ions release. [39, 40]

Anti-bacterial activity of nanoparticles is assigned to water absorption on the surface of tungsten oxide nanoparticles as a layer of full H$^+$ions which contacts the bacteria and damages their membrane.

Measuring the apoptotic potential of WO₃ nanoparticles by flow cytometry

The apoptotic WO₃ nanoparticles effect on AGS cells and PBMCs was determined by using the Annexing-V-FITC/PI dual staining method. Share of early apoptosis and late apoptotic has been showed in the Fig. 6. These results were obtained in the optimal concentration of nanoparticles and 4 days after the radiation.

The cells of AGS control group became 1.75% apoptosis and 1.1% necrosis. But for dose 8 Gy (radiation alone), the percentage of apoptosis and necrosis were 81.6% and 69.74%, respectively which had noticeable growth. These values were 15.82% and 12.44% for the NPs group of PBMCs without radiation, respectively (Fig. 6). The results of flow cytometer showed that the percentage of apoptosis and necrosis cells will be increased remarkably by raising the radiation dose.

In all the cases, apoptosis and necrosis share of cells exposed to nanoparticles and the radiation, was more than a situation with the lonely radiation.

Large numbers of necrosis and apoptosis cells in high doses show that these two factors have an important role in radio sensitization. We used MTT assays for examining the toxicity of WO₃ NPs. But this method has some weaknesses. For example, MTT assays can't distinguish necrosis cells and apoptosis from the normal cells and can't specify the mechanisms of cell death.
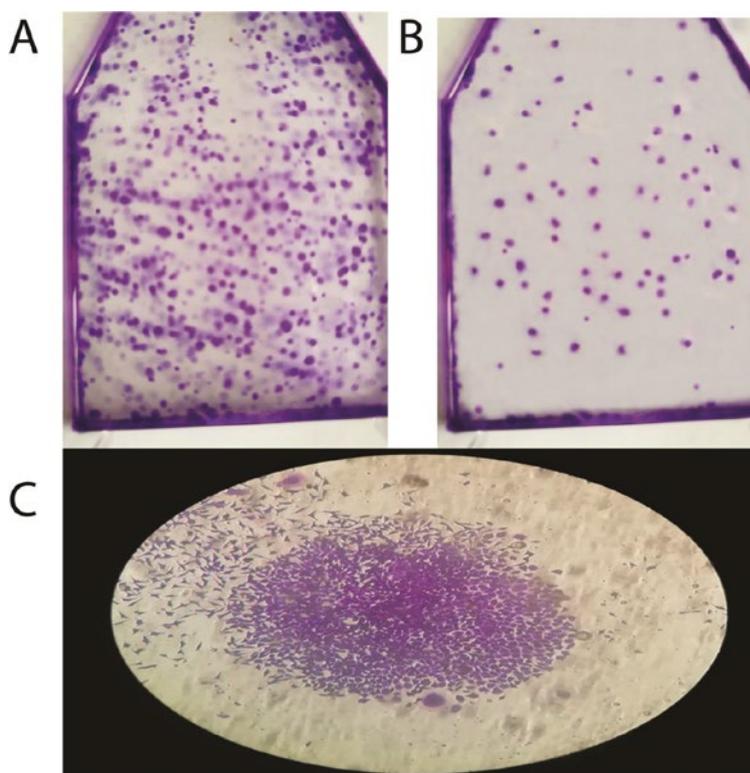

Fig. 7. The tungsten oxide NPs affects colony formation of AGS cells in combination with radiation. The cells followed by 2,4,6 and 8 Gy of irradiation, treated with or without 89.6 µg/mL WO₃ NPs, the control group and 8 Gy group without WO₃ NPs have been shown in (A) and (B) .(C) Representative colony of AGS cells in clonogenic assay of AGS cells treated with WO₃ NPs

When cancer cells start to apoptosis by the nanoparticles effect, the normal cells will be necrosis if the nanoparticles is toxic. Using this toxicity of nanoparticles mechanism is examined for clinical usage.

Radio sensitizing efficacies of WO₃ NPs

In vitro tests were performed for examining the effect of radio sensitization of WO₃ NPs on AGS cell line (Fig. 7A-C). The cells were exposed to nanoparticles with the optimal concentration. Primarily, clonogenic assay is as the gold standard for
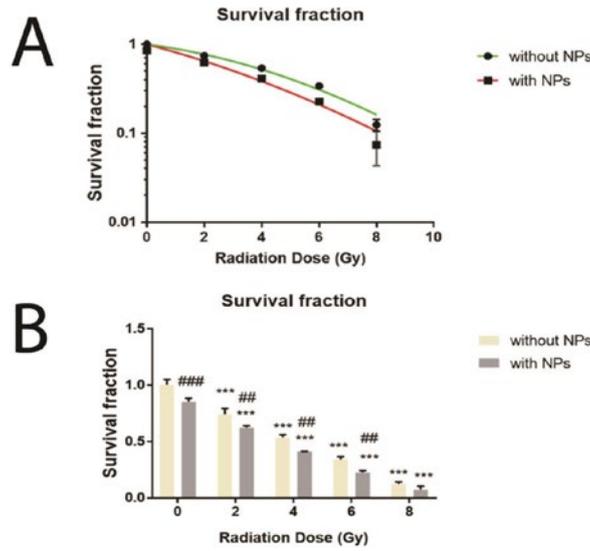

Fig. 8. In vitro radio sensitization effect of WO₃ NPs in AGS cells. (A) Clonogenic assay of AGS cells were treated with 2, 4, 6 and 8 Gy of irradiation in combination with WO₃ NPs or without; (B) the histogram figures are survival fraction of colonies quantified. Data is a summary of three independent experiments and expressed as mean ± SD. *$P<0.05$, **$P<0.01$, ***$P<0.001$ compared with the control group. #$P<0.05$, ##$P<0.01$, ###$P<0.001$ compared with the corresponding WO₃ NPs-treated group.
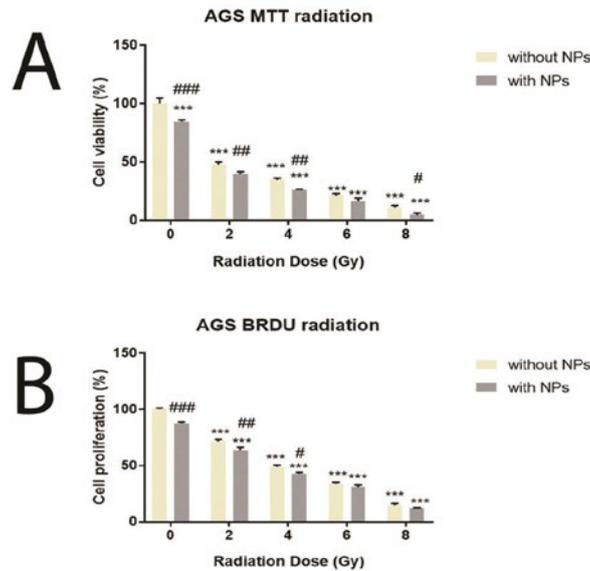

Fig. 9. The tungsten oxide NPs affects AGS cell viability (A) and proliferation (B). The cells followed by 2, 4, 6 and 8 Gy of irradiation .The cells have been incubated in 89.6 µg/mL concentration of WO₃ NPs for 24 hours. Cell viability and cell proliferation have been determined 7 days after radiation treatment by using an MTT assay and BrdU assay, respectively. Data is a summary of three independent experiments and expressed as mean ± SD. *$P<0.05$, **$P<0.01$, ***$P<0.001$ compared with the control group. #$P<0.05$, ##$P<0.01$, ###$P<0.001$ compared with the corresponding WO₃ NPs-treated group.

specifying radio sensitization. As in the Fig. 8A Fig. 8B), the survival fraction has been decreased remarkably by increasing dose. The DEF and SER indexes were measured 1.68 and 1.24 respectively. The extracted α and β parameters from the linear quadratic curves were 0.09852 ± 0.01914 Gy^{-1} and 0.01616 ± 0.003738 Gy^{-2} for the control sample (radiation lonely) and 0.1972 ± 0.04451 Gy^{-1} and 0.01047 ± 0.009228 Gy^{-2} for the cells with WO₃ NPs, respectively.

MTT assay (Fig. 9A) operated on AGS cells has approved the radio sensitization capability of WO₃ NPs so that the cell viability has been decreased 8.42% in dose 4 Gy relative to the correspondent group (radiation lonely). Radiation exposure prohibited the cell proliferation (Fig. 9B). It reduced the ability of DNA proliferation. This reduction were more by increasing the radiation dose. So, in dose 4 Gy with NPs, the proliferation capability was decreased 57.2% than the group control. This reduction had a more relative increase for the groups including nanoparticles than the lonely radiation group. In dose 2 Gy, the group including nanoparticles and radiation had 7.78% reduction in proliferation capability than the correspondent radiation group without nanoparticles.

It was improved that DEF has more Kilo voltage energies than megavoltage energies. But low range of kilo voltage energies and also their non-uniform distribution in tumor prohibit using this energy clinically [41]. Megavoltage energies have limitations but we can use them in nanoparticle-based radiotherapy.

It's supposed that secondary electrons produced by the radiation of megavoltage as well as nanoparticles cause to create extra low range secondary electron that these electrons produce free radical and by this way, they can raise the treatment output [42, 43]. The overview of up-to-date NP-mediated enhancement factors used in clonogenic studies literature is given in Table 1.

Table 1. Overview of modifying enhancement ratios used in nanoparticles studies

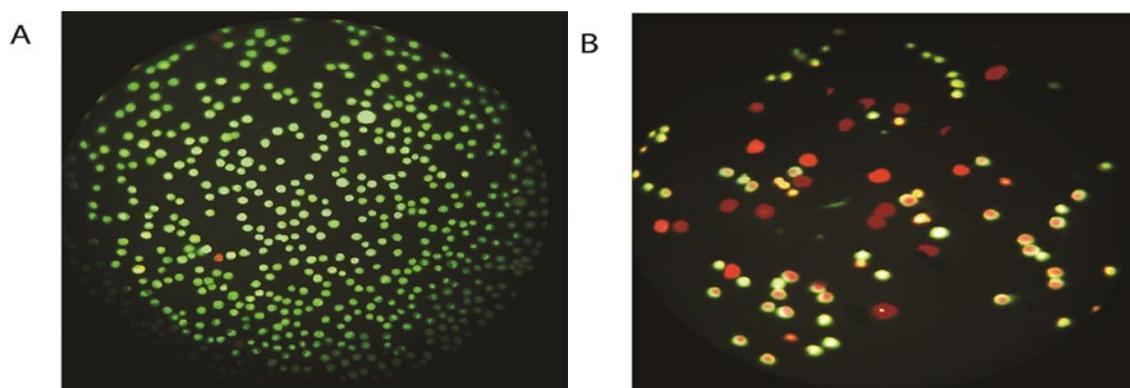| Cell line	Radiation sourse	NPs(size)	Notes	Reference
GES-1 BGC823 SGC7901 MKN45	4 MeV electrons	DOC-NP (85nm)	The SER values of DOC-NPs significantly increased in three GC cell lines (increased 1.09-fold to 1.24-fold, **P < 0.01) but elevated slightly in GES-1cells (1.02-fold, P = 0.38).	[44]
HeLa	Co-60	Au-NP (50 nm)	DEF was determined 1.05 ± 0.02 for Folate-conjugated GNPs and 1.03 ± 0.01 for Pegylated GNPs.	[45]
Panc1	6 MV X-rays	AGuIX-NP	The SER₄Gy is 1.20 ± 0.04 for the FFF irradiation and 1.12 ± 0.04 for the STD. The DEF20 % is 1.30 ± 0.05 for the FFF and 1.23 ± 0.03 for the STD.	[46]
MDA-MB-231	6 MV	Glu-Au-NP(16nm)	The curves also show that 49-nmGlu-GNPs induce stronger radio sensitivity than 16-nm Glu-GNPs with SERs of 1.86 and 1.49, respectively (P<0.05).	[47]
9L Gliosarcoma	10MV	Bi₂O₃ (50-70nm)	Sensitization enhancement ratios of 1.48 and 1.25 for 125 kVp and 10 MV were obtained in vitro,respectively.	[48]

Fig. 10. The AGS cells were stained by AO/EB and observed under fluorescence microscope.
A) (Control group of AGS cells): The circular nucleus is uniformly distributed in the cell center. Experimental group (early apoptosis cells): the nucleus showed yellow-green fluorescence by Acridine Orange (AO) staining and concentrated into a crescent or granular placed in one side of cells.
B) Experimental group (secondary apoptotic cells): the cell nucleus suggested orange fluorescence by EB staining and had been gathered in concentration and placed in bias. Necrotic cells: The volume of necrosis cells showing uneven orange-red fluorescence and an unapparent outline, was increased. It will be dissolved or closed to disintegration.
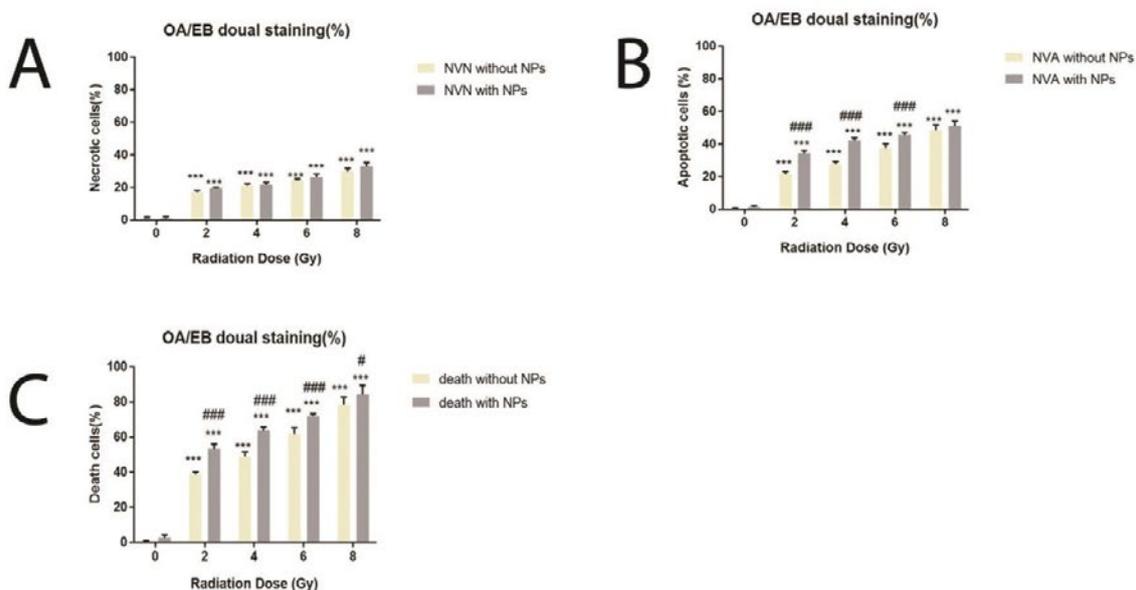
Fig. 11. AO/EB double staining analysis shows the apoptotic rate of AGS cells. The AGS cells followed by 2, 4, 6 and 8 Gy of irradiation have treated with or without 89.6 µg/mL WO₃ NPs. Histograms show A Necrotic index, B Apoptotic index and C Percentage dead cells based on AO/EB stained cells.
Data is a summary of three independent experiments and expressed as mean ± SD. *$P<0.05$, **$P<0.01$, ***$P<0.001$ compared with the control group. #$P<0.05$, ##$P<0.01$, ###$P<0.001$ compared with the corresponding WO₃ NPs-treated group

Acridine orange/ethidium bromide staining

By using Fluorescence microscope, Acridine orange/ethidium bromide staining showed that the color of normal cells is green uniformly, while the cells involved early apoptosis were oserved with green color or yellowish and dense chromatin. The Fig. 10 (A and B) shows AGS cells involved apoptosis and necrosis by using Acridine orange/ ethidium bromide staining. The necrosis cells were specified by red color and disrupted nucleus and late apoptotic cells with orange color and dense chromatin and willing to one side of cell. The used concentration of nanoparticles was the optimal concentration. Doses of 2, 4, 6 and 8 were used. The percentage of cells' necrosis and apoptosis has been increased noticeably by raising dose. It also happens in the groups having nanoparticles more than the groups without nanoparticles after the radiation of apoptosis and necrosis (Fig. 11 A-C). The death percentage of AGS cells including nanoparticles which received dose 6 Gy was 71.2% more than the control group and 10.13% more than the correspondent group without nanoparticles.

Dual AO/EB fluorescent staining can specify the apoptosis, necrosis and early and late apoptosis cells according to the cell shape and color.

AO in normal cells and the cells which have been early apoptosis will be penetrated, while their membrane is complete and will be connect to DNA. They are green under the microscope. EB will just penetrate in cells which their membrane has been damaged like the late apoptosis and necrosis and will be connected to the parts of DNA which will be seen orange or red.

CONCLUSION

This study tried to review the toxicity potential of WO₃ NPs on AGS cell line and its mechanisms. The toxicity effects of WO₃ NPs whose size is 31.89±3.82 nm caused to reduce cell survival and damage DNA in the concentrations more than 100 µg/mL.

In this study the radio sensitization potential of WO₃ NPs was examined and it was determined that WO₃ NPs has the ability in radio sensitization because of high capability of nanoparticles in radiation absorption and production of secondary electrons .This capability was examined by using MTT assay, BrdU assay and clonogenic assay.

The small size, large surface area and the ions of WO₃ NPs were participated in creating toxicity. The effects of toxic and genotoxic WO₃ NPs depended on both nanoparticles concentration and the time

for exposing cells to the nanoparticles.

Any damages to DNA and reduction of cell survival related to increase oxidative stress and inflation resulted from increasing ROS production led to apoptosis and change the cell form.

Our studies show that the main model for death was apoptosis which has been created by the accumulation of ROS and activation of caspase-9 and -3.

ACKNOWLEDGMENTS

CONFLICT OF INTEREST

The authors declare that there are no conflicts of interest regarding the publication of this manuscript.

REFERENCES

1. Kamel SI, De Jong MC, Choti MA, Hirose K, Wolfgang CL, Edil BH, et al. The Role Of Liver Directed Surgery In Patients With Hepatic Metastasis From A Gynecologic Primary Carcinoma: A Comprehensive Single-Institution Study of 87 Patients. Journal of Surgical Research. 2011;165(2):338.

2. Manthe RL, Foy SP, Krishnamurthy N, Sharma B, Labhasetwar V. Tumor Ablation and Nanotechnology. Molecular Pharmaceutics. 2010;7(6):1880-98.

3. Jemal A, Bray F, Center MM, Ferlay J, Ward E, Forman D. Global cancer statistics. CA: A Cancer Journal for Clinicians. 2011;61(2):69-90.

4. Jemal A, Siegel R, Xu J, Ward E. Cancer Statistics, 2010. CA: A Cancer Journal for Clinicians. 2010;60(5):277-300.

5. Hoffelt SC. Gamma Knife vs. CyberKnife. Oncology Issues. 2006;21(5):18-20.

6. Bump EA, Hoffman SJ, Foye WO. Radiosensitizers and Radioprotective Agents. Burger's Medicinal Chemistry and Drug Discovery: John Wiley & Sons, Inc.; 2003.

7. Javvadi P, Segan AT, Tuttle SW, Koumenis C. The Chemopreventive Agent Curcumin Is a Potent Radiosensitizer of Human Cervical Tumor Cells via Increased Reactive Oxygen Species Production and Overactivation of the Mitogen-Activated Protein Kinase Pathway. Molecular Pharmacology. 2008;73(5):1491-501.

8. Jain S, Coulter JA, Hounsell AR, Butterworth KT, McMahon SJ, Hyland WB, et al. Cell-Specific Radiosensitization by Gold Nanoparticles at Megavoltage Radiation Energies. International Journal of Radiation Oncology*Biology*Physics. 2011;79(2):531-9.

9. Sharma V, Shukla RK, Saxena N, Parmar D, Das M, Dhawan A. DNA damaging potential of zinc oxide nanoparticles in human epidermal cells. Toxicology Letters. 2009;185(3):211-8.

10. Le Sech C, Kobayashi K, Usami N, Furusawa Y, Porcel E, Lacombe S. Comment on 'Therapeutic application of metallic nanoparticles combined with particle-induced x-ray emission effect'. Nanotechnology. 2012;23(7):078001.

11. Kaliberov SA, Buchsbaum DJ. Cancer Treatment with Gene Therapy and Radiation Therapy. Applications of viruses for cancer therapy: Elsevier; 2012. p. 221-63.

12. Liu H, Ma L, Liu J, Zhao J, Yan J, Hong F. Toxicity of nano-anatase TiO2to mice: Liver injury, oxidative stress. Toxicological & Environmental Chemistry. 2010;92(1):175-86.

13. Lai JC, Lai MB, Jandhyam S, Dukhande VV, Bhushan A, Daniels CK, et al. Exposure to titanium dioxide and other metallic oxide nanoparticles induces cytotoxicity on human neural cells and fibroblasts. International journal of nanomedicine. 2008;3(4):533.

14. Zheng Y, Hunting DJ, Ayotte P, Sanche L. Radiosensitization of DNA by Gold Nanoparticles Irradiated with High-Energy Electrons. Radiation Research. 2008;169(1):19-27.

15. Pan Y, Neuss S, Leifert A, Fischler M, Wen F, Simon U, et al. Size-Dependent Cytotoxicity of Gold Nanoparticles. Small. 2007;3(11):1941-9.

16. Yuan S-J, He H, Sheng G-P, Chen J-J, Tong Z-H, Cheng Y-Y, et al. A Photometric High-Throughput Method for Identification of Electrochemically Active Bacteria Using a WO3 Nanocluster Probe. Scientific Reports. 2013;3(1).

17. Anithaa AC, Lavanya N, Asokan K, Sekar C. WO3 nanoparticles based direct electrochemical dopamine sensor in the presence of ascorbic acid. Electrochimica Acta. 2015;167:294-302.

18. Ivask A, Titma T, Visnapuu M, Vija H, Kakinen A, Sihtmae M, et al. Toxicity of 11 Metal Oxide Nanoparticles to Three Mammalian Cell Types *In V.itro*. Current Topics in Medicinal Chemistry. 2015;15(18):1914-29.

19. Kwon HJ, Shin K, Soh M, Chang H, Kim J, Lee J, et al. Large-Scale Synthesis and Medical Applications of Uniform-Sized Metal Oxide Nanoparticles. Advanced Materials. 2018;30(42):1704290.

20. Snyder RA, Castaldo ET, Bailey CE, Phillips SE, Chakravarthy AB, Merchant NB. Survival Benefit of Adjuvant Radiation Therapy for Gastric Cancer following Gastrectomy and Extended Lymphadenectomy. International Journal of Surgical Oncology. 2012;2012:1-7.

21. Fubini B, Ghiazza M, Fenoglio I. Physico-chemical features of engineered nanoparticles relevant to their toxicity. Nanotoxicology. 2010;4(4):347-63.

22. Murdock RC, Braydich-Stolle L, Schrand AM, Schlager JJ, Hussain SM. Characterization of Nanomaterial Dispersion in Solution Prior to In Vitro Exposure Using Dynamic Light Scattering Technique. Toxicological Sciences. 2007;101(2):239-53.

23. Kisin ER, Murray AR, Keane MJ, Shi X-C, Schwegler-Berry D, Gorelik O, et al. Single-walled Carbon Nanotubes: Geno- and Cytotoxic Effects in Lung Fibroblast V79 Cells. Journal of Toxicology and Environmental Health, Part A. 2007;70(24):2071-9.

24. Warheit DB. How Meaningful are the Results of Nanotoxicity Studies in the Absence of Adequate Material Characterization? Toxicological Sciences. 2008;101(2):183-5.

25. Magdolenova Z, Collins A, Kumar A, Dhawan A, Stone V, Dusinska M. Mechanisms of genotoxicity. A review ofin vitroandin vivostudies with engineered nanoparticles. Nanotoxicology. 2013;8(3):233-78.

26. Li Y, Sun L, Jin M, Du Z, Liu X, Guo C, et al. Size-dependent cytotoxicity of amorphous silica nanoparticles in human hepatoma HepG2 cells. Toxicology in Vitro.

2011;25(7):1343-52.

27. Prajapati MV, Adebolu OO, Morrow BM, Cerreta JM. Original Research: Evaluation of pulmonary response to inhaled tungsten (IV) oxide nanoparticles in golden Syrian hamsters. Experimental Biology and Medicine. 2016;242(1):29-44.

28. Ahamed M, Akhtar MJ, Khan MAM, Alhadlaq HA, Aldalbahi A. Nanocubes of indium oxide induce cytotoxicity and apoptosis through oxidative stress in human lung epithelial cells. Colloids and Surfaces B: Biointerfaces. 2017;156:157-64.

29. Ahamed M, Khan MAM, Akhtar MJ, Alhadlaq HA, Alshamsan A. Role of Zn doping in oxidative stress mediated cytotoxicity of TiO2 nanoparticles in human breast cancer MCF-7 cells. Scientific Reports. 2016;6(1).

30. Patel P, Kansara K, Senapati VA, Shanker R, Dhawan A, Kumar A. Cell cycle dependent cellular uptake of zinc oxide nanoparticles in human epidermal cells. Mutagenesis. 2016;31(4):481-90.

31. Senapati VA, Jain AK, Gupta GS, Pandey AK, Dhawan A. Chromium oxide nanoparticle-induced genotoxicity and p53-dependent apoptosis in human lung alveolar cells. Journal of Applied Toxicology. 2015;35(10):1179-88.

32. Turkez H, Sonmez E, Turkez O, Mokhtar YI, Stefano AD, Turgut G. The Risk Evaluation of Tungsten Oxide Nanoparticles in Cultured Rat Liver Cells for Its Safe Applications in Nanotechnology. Brazilian Archives of Biology and Technology. 2014;57(4):532-41.

33. Kononenko V, Repar N, Marušič N, Drašler B, Romih T, Hočevar S, et al. Comparative in vitro genotoxicity study of ZnO nanoparticles, ZnO macroparticles and ZnCl 2 to MDCK kidney cells: Size matters. Toxicology in Vitro. 2017;40:256-63.

34. Jänicke RU, Sprengart ML, Wati MR, Porter AG. Caspase-3 Is Required for DNA Fragmentation and Morphological Changes Associated with Apoptosis. Journal of Biological Chemistry. 1998;273(16):9357-60.

35. Ortega R, Bresson C, Darolles C, Gautier C, Roudeau S, Perrin L, et al. Low-solubility particles and a Trojan-horse type mechanism of toxicity: the case of cobalt oxide on human lung cells. Particle and Fibre Toxicology. 2014;11(1):14.

36. Papis E, Rossi F, Raspanti M, Dalle-Donne I, Colombo G, Milzani A, et al. Engineered cobalt oxide nanoparticles readily enter cells. Toxicology Letters. 2009;189(3):253-9.

37. Chen Q, Thouas GA. Metallic implant biomaterials. Materials Science and Engineering: R: Reports. 2015;87:1-57.

38. Vandebriel R, De Jong W. A review of mammalian toxicity of ZnO nanoparticles. Nanotechnology, Science and Applications. 2012:61.

39. Ganesan R, Gedanken A. Synthesis of WO3nanoparticles using a biopolymer as a template for electrocatalytic hydrogen evolution. Nanotechnology. 2007;19(2):025702.

40. Syed MA, Manzoor U, Shah I, Bukhari SHA. Antibacterial effects of Tungsten nanoparticles on the Escherichia coli strains isolated from catheterized urinary tract infection (UTI) cases and Staphylococcus aureus. New Microbiologica. 2010;33(4):329-35.

41. Verhaegen F, Reniers B, Deblois F, Devic S, Seuntjens J, Hristov D. Dosimetric and microdosimetric study of contrast-enhanced radiotherapy with kilovolt x-rays. Physics in Medicine and Biology. 2005;50(15):3555-69.

42. Liu J, Liang Y, Liu T, Li D, Yang X. Anti-EGFR-Conjugated Hollow Gold Nanospheres Enhance Radiocytotoxic Targeting of Cervical Cancer at Megavoltage Radiation Energies. Nanoscale Research Letters. 2015;10(1).

43. Meidanchi A, Akhavan O, Khoei S, Shokri AA, Hajikarimi Z, Khansari N. ZnFe2O4 nanoparticles as radiosensitizers in radiotherapy of human prostate cancer cells. Materials Science and Engineering: C. 2015;46:394-9.

44. Cui F-b, Li R-T, Liu Q, Wu P-y, Hu W-j, Yue G-f, et al. Enhancement of radiotherapy efficacy by docetaxel-loaded gelatinase-stimuli PEG-Pep-PCL nanoparticles in gastric cancer. Cancer Letters. 2014;346(1):53-62.

45. Khoshgard K, Hashemi B, Arbabi A, Rasaee MJ, Soleimani M. Radiosensitization effect of folate-conjugated gold nanoparticles on HeLa cancer cells under orthovoltage superficial radiotherapy techniques. Physics in Medicine and Biology. 2014;59(9):2249-63.

46. Detappe A, Kunjachan S, Rottmann J, Robar J, Tsiamas P, Korideck H, et al. AGuIX nanoparticles as a promising platform for image-guided radiation therapy. Cancer Nanotechnology. 2015;6(1).

47. Wang C, Jiang Y, Li X, Hu L. Thioglucose-bound gold nanoparticles increase the radiosensitivity of a triple-negative breast cancer cell line (MDA-MB-231). Breast Cancer. 2013;22(4):413-20.

48. Stewart C, Konstantinov K, McKinnon S, Guatelli S, Lerch M, Rosenfeld A, et al. First proof of bismuth oxide nanoparticles as efficient radiosensitisers on highly radioresistant cancer cells. Physica Medica. 2016;32(11):1444-52.